Available online at www.sciencedirect.com
ScienceDirect
Journal of Nuclear Materials 372 (2008) 233–238
journal of nuclear materials
www.elsevier.com/locate/jnucmat

Simulation of diffusion of oxygen and uranium in uranium dioxide nanocrystals

A.Ya. Kupryazhkin [a,*], A.N. Zhiganov [a], D.V. Risovany [a], K.A. Nekrassov [a], V.D. Risovany [b], V.N. Golovanov [b]

[a] *Ural State Technical University, 620002, Mira Street 19, Yekaterinburg, Russia*
[b] *Research Institute of Atomic Reactors, 433510 Dimitrovgrad, Ulyanovsk region, Russia*

Received 24 October 2006; accepted 15 March 2007

Abstract

The method of molecular dynamics is used to study phase transitions and ion transport phenomena in uranium dioxide nanocrystals. The temperature dependences of uranium and oxygen diffusion coefficients in the range from 2280 to 3950 K are calculated separately for surface, near-surface and bulk regions of the crystals. On these dependences we have distinguished temperature intervals, which correspond to crystalline phase, superionic state and melt. The activation energies of diffusion and pre-exponential factors for these intervals are determined. The obtained results are compared with experimental data and calculations of other authors.

1. Introduction

Complexity of the problem of prediction of transport phenomena in uranium oxide fuel of nuclear reactors during the processes of fuel manufacturing and exploitation requires the development of independent approaches to the analysis of diffusion of oxygen and uranium ions in uranium dioxide on microscopic scales. It is attractive to accomplish such analysis using the method of molecular dynamics (MD). This method has already been used to study the oxygen diffusion in UO_2 [1–3] and individual properties of the oxide fuel. However, in spite of a number of essential results acquired before, there are problems which remain not adequately investigated, including the oxygen behavior in the superionic transition region and perspectives of MD-simulation of uranium self-diffusion in UO_2 crystals. There is also interest in the development of simulation methods of uranium dioxide nanocrystals, because of their unique characteristics and use of the nanocrystals in the technology of fabrication of ceramic fuel [4].

2. Molecular dynamics simulation procedure

To simulate UO_2 crystals, we applied the ionic model, in which a crystal consists of doubly-charged oxygen anions and four-charged uranium cations. Both integer-valued and fractional charges of the ions have been examined. Interactions between the ions were described with pair interaction potentials $U(r_{ij})$ of the form

$$U(r_{ij}) = k_e \frac{z_i z_j e^2}{r_{ij}} + A_{ij} \cdot \exp(-B_{ij} r_{ij}) - \frac{C_{ij}}{r_{ij}^6}, \quad (1)$$

where i, j are numbers of the interacting ions, $z_i e$, $z_j e$ are their charges, r_{ij} is the distance between the ions, A_{ij}, B_{ij} and C_{ij} are parameters of the short-range interaction.

In this work, we have considered two sets of the short-range interaction potentials, both taken from Walker and Catlow [5]. Parameters for these sets are listed in Table 1. Potentials No. 1 directly take into account polarization of the electron shells and so are expected to be more suitable for the rigid-ion model used in this work. Potentials No. 2 were designed to be used with the shell model and so do not take account of the polarization.

* Corresponding author. Tel.: +7 8 343 3754146.
E-mail address: kupr@dpt.ustu.ru (A.Ya. Kupryazhkin).

0022-3115/$ - see front matter © 2007 Elsevier B.V. All rights reserved.
doi:10.1016/j.jnucmat.2007.03.176

Table 1
Parameters of the non-Coulomb part of the particle interaction potentials for UO_2 [5][a]

No.	Potential parameter	A (eV)	B (10^{10} m^{-1})	C (eV 10^{-60} m^6)
1	U–O	873.327	2.4771	0.0
	O–O	50259.3	6.5424	72.65
2	U–O	1297.44	2.6688	0.0
	O–O	22764.3	6.7114	20.37

[a] Potentials No. 1 directly take into account polarization of the electron shells. Potentials No. 2 were designed to be used with the shell model and so do not take account of the polarization directly.

The Euler method with half-step was used to solve numerically the equations of motion of the particles, the magnitude of time step being equal to 5×10^{-15} s. Simulations were carried out under zero boundary conditions, i.e. for cubic nanocrystals in vacuum. The maximum number of ions in the model crystals was 8768. In all calculations, stoichiometry was assumed.

The model crystallites were divided into three regions, namely surface, near-surface and bulk zones. The surface zone had a thickness of one lattice parameter a, which at room temperature is equal to 0.547 nm. The near-surface zone was situated immediately under the surface zone and had the same thickness one lattice parameter. Remaining inner volume was included into the bulk zone, which was used to describe the behavior of ions in the bulk of crystal. For the most-used crystal of 6144 ions the bulk zone had linear size of $4a$ containing 768 ions. The surface and near-surface zones for crystal of this size contain 3552 and 1824 ions, respectively.

The diffusion coefficients D_{eff} of anions and cations for a given temperature were calculated using the Einstein formula for the dependence of the mean square displacement of the ions $\langle \Delta r^2 \rangle$ on time t

$$\lim_{t\to\infty} \langle \Delta r^2 \rangle = 6 D_{\text{eff}} t + \text{const}. \quad (2)$$

The mean square displacements of the ions were calculated using the relation

$$\langle \Delta r^2 \rangle_\alpha = \frac{1}{N_\alpha} \sum_{i\in\alpha} |\mathbf{r}_i^n - \mathbf{r}_i^0|^2. \quad (3)$$

Here, the summation is over N_α particles of kind α for the n-th time step.

Disordering in the model crystals was studied from the character of behavior of the corresponding pair radial functions

$$g(r) = \frac{V}{N} \frac{N(r, \Delta r)}{4\pi r^2 \Delta r}. \quad (4)$$

Here, $N(r, \Delta r)$ is the number of particles in the spherical layer of thickness Δr at distance r from the considered ion, V is the volume of the simulated crystallite, N is the number of particles in it.

3. Experimental results and discussion

Melting temperatures of UO_2 nanocrystals calculated in this work using MD are shown in Fig. 1. These temperatures correspond to different sizes of the crystals and two types of potentials from [5], both with full integer charges of U^{4+} and O^{2-} ions. As it follows from the given results, the most real melting temperature has been obtained using the set of potentials No. 1 ((Table 1), ([5])), which takes into account the polarization of ions. Therefore, all the subsequent MD calculations in this work were carried out using this set. It is necessary to notice, that according to the calculations (Fig. 1), change of the UO_2 crystal size from 2.2 up to 4.9 nm leads to the change of the melting temperature by 1500 K.

We have registered a sharp change in density of UO_2 nanocrystals at the melting point, as it is shown in Fig. 2. The calculated change of density of the molten UO_2 crystal (≈9.6%) is in good agreement with experimental data (see, for example, [6]).

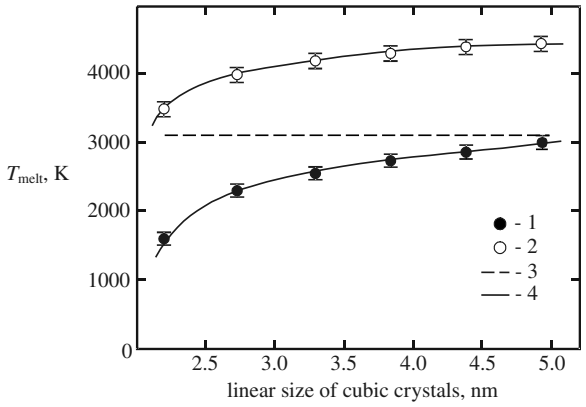

Fig. 1. Melting temperatures for model UO_2 nanocrystals of various sizes. 1 – simulation with potentials, which directly take into account polarization of the electron shells (No. 1 in Table 1); 2 – potentials, requiring use of the shell model to take account of the polarization (No. 2 in Table 1); 3 – experimental value of the uranium dioxide melting temperature $T_{\text{melt}} = 3120$ K; and 4 – approximations.

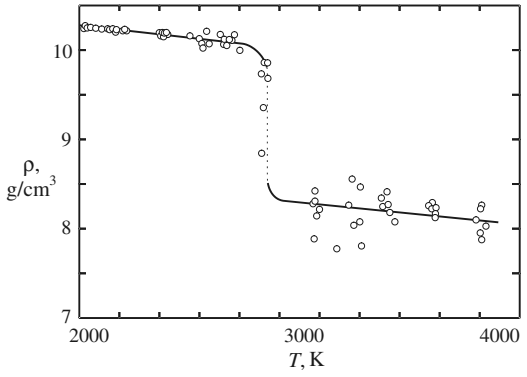

Fig. 2. Typical dependence of the model crystals density ρ on temperature. Zero border conditions, 8748 particles. For crystals of this size the calculated melting temperature was ≈2990 K (see Fig. 1).

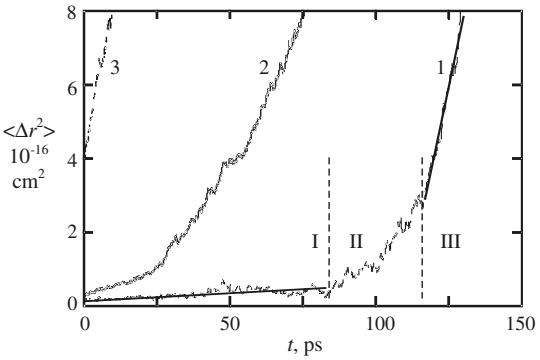

Fig. 3. Dependence of the mean square ion displacements in UO_2 on time in process of melting. $T = 3120$ K. 1 – uranium ions in the bulk zone; 2 – uranium ions in the near-surface zone; 3 – oxygen ions in the bulk region; straight solid lines are approximations. I–III are sections of the curve 1, corresponding to metastable crystal phase, transition region and the melt, respectively.

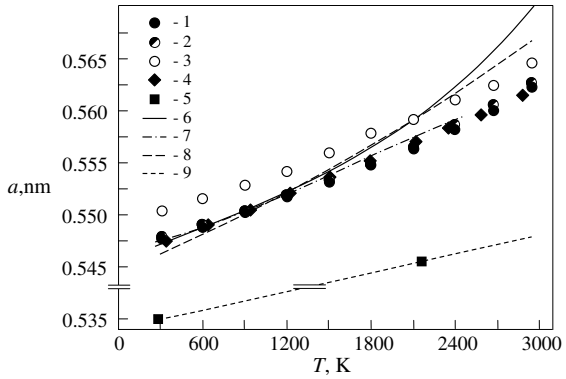

Fig. 4. Dependences of the lattice parameter of the model crystals on temperature. 1 – this work, nanocrystal bulk, $q_- = -1.9085e$, potentials No. 1 in Table 1, zero border conditions; 2 – the same conditions, near-surface region; 3 – the same conditions, surface region; 4 – the same charges and potentials as for points 1–3, but with periodical border conditions suggested by Ryabov in [8]; 5 – the same short-range potentials as for points 1–4, zero border conditions, integer ion charges ($q_- = -2e$); 6 – experimental data from [7] in temperature range 300 K $\leqslant T \leqslant$ 3100 K; 7 – MD modeling in [3] using an alternative set of potentials, suggested in that work, where $q_- = -1.2e$; 8 – MD modeling in [1] with another alternative set of potentials, $q_- = -1.6e$; and 9 – approximation of points 5.

Typical time dependences of the mean square displacements of ions in the model crystallites are shown in Fig. 3. The curves correspond to uranium ions in the bulk and near-surface (denoted as 1 and 2, respectively) zones, and to oxygen ions in the bulk zone (as 3) at $T = 3120$ K, slightly exceeding the melting temperature of the model crystallites (see Fig. 1). The dependence No. 1 for uranium cations in the bulk zone can be divided into three sections. Two of these sections (I, III) are linear, corresponding to uranium diffusion in the crystal phase (metastable state) and in the melt, accordingly. Thus, with the consideration of the metastable states at temperatures exceeding the melting temperature, it is possible to obtain two values of the ion diffusion coefficients corresponding to different phase states of uranium dioxide on the same curve. Section II of the curve No. 1 corresponds to partially molten crystals. As we have observed, the process of melting started at surface of crystal and then zone of the melt gradually grew up towards the center.

Fig. 4 shows the temperature dependences of the uranium dioxide lattice parameter for a number of potential sets in comparison with experimental data [7]. As it follows from the figure, in spite of the fact, that potentials [5] give satisfactory prediction of the melting temperature (Fig. 1) and the change of density at the melting point, these potentials give a UO_2 lattice parameter underestimated by 20 pm (≈2%, see Fig. 4). To remove this discrepancy, in the present work effective charges of uranium and oxygen ions have been lowered from $+4e$ and $-2e$ to $+3.817e$ and $-1.9085e$, respectively. This has led to the required increase of the lattice parameter in the bulk zone of the model UO_2 nanocrystals. Temperature dependence of the lattice parameter calculated with the modified charges within the uncertainty limits coincides with the dependence received for an infinite crystal (periodic border conditions [8], curve 4 in Fig. 4). This coincidence allows, using results of modeling of the bulk zone of nanocrystals, to determine the characteristics of usual crystals also.

Values of the UO_2 lattice parameter calculated for the near-surface region are slightly above the values in the bulk, and values of the period in the surface layer are even higher, exceeding the bulk values by 3 pm (≈0.6%). It is necessary to note also, that the reduction of ion charges has led to the concurrence of our lattice parameter values to data of work [3] (curve 7 in Fig. 4) obtained with an alternative set of ion interaction potentials. The period values are, as well, in satisfactory agreement with calculations [1] carried out with another alternative potential set (curve 8 in Fig. 4). At high temperatures ($T > 1500$ K) all the examined potentials give values of the lattice parameter underestimated in comparison with the experiment.

A reduction of the ion charges in this work has led to increase of the melting temperature of the crystal. Therefore, in the following calculations of ion diffusion coefficients, potentials with the lowered charges were used only up to temperatures not exceeding $T = 3100$ K.

Analysis of dependences of mean square displacements of the ions on time $\langle \Delta r^2 \rangle = f(t)$ has allowed us to obtain values of the coefficients of ion diffusion for a number of temperatures. The calculated temperature dependences of the oxygen self-diffusion coefficients in the bulk, near-surface and surface zones of UO_2 nanocrystals are shown in Fig. 5. As it follows from these data, the dependence $\ln D_{\text{eff}} = f(T)$ for the bulk region (curves 3, 6, 9, 10 in Fig. 5) has three different reliably distinguished temperature intervals. For the other zones of the crystallite there are two temperature intervals. In all the zones the high-temperature interval (at $T > 3100$ K) corresponds to the UO_2 melt.

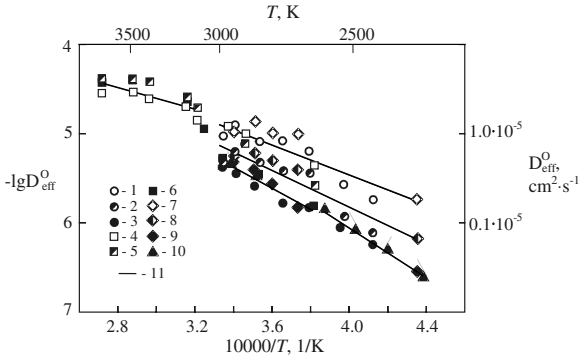

Fig. 5. Dependences of the oxygen diffusion coefficients on temperature. 1, 4, 7 – crystal surface zone; 2, 5, 8 – the near-surface zone; 3, 6, 9, 10 – the bulk zone; 1–6 – 6144 ions; 7–10 – 4116 ions; 1–3, 10 – fractional charges, $q_- = -1.9085e$; 4–9 – integer charges, $q_- = -2e$; and 11 – approximations.

For each of the temperature intervals in all the three zones the oxygen diffusion coefficients are described by the Arrhenius dependence

$$D_{\text{eff}} = D_{0\text{eff}} \cdot \exp\left\{-\frac{\Delta E^{\text{O}}_{\text{eff}}}{kT}\right\}. \tag{5}$$

The values of the diffusion coefficients obtained for different charges of ions and numbers of ions in the nanocrystals are within the limits of modeling errors (Fig. 5). Therefore, we handled the curves $\ln D_{\text{eff}} = f(1/T)$ for all the data received with different charges and numbers of particles jointly. Calculated values of the pre-exponential factors $D_{0\text{eff}}$ and the diffusion activation energies $\Delta E^{\text{O}}_{\text{eff}}$ are given in Table 2. For comparison, in the same table the experimental data obtained by other authors for lower temperatures are shown.

To determine the nature of change in the oxygen bulk diffusion coefficient from (2.76 ± 0.13) eV at $T = (2280-2600)$ K to (2.34 ± 0.23) eV at $T = (2624-3080)$ K and to (1.24 ± 0.32) eV at $T > 3100$ K, we studied the behavior of the oxygen–oxygen radial distribution function $g_{\text{o–o}}(r)$. As it follows from these data, at low temperatures ($T = 300$ K) in the oxygen sublattice of the nanocrystal bulk there is long-range ordering corresponding to the crystalline phase, which is evident from the sharp $g_{\text{o–o}}(r)$ peaks corresponding to the different coordination spheres. Approaching $T = 2600$ K, peak broadening is observed, and after $T = 2600$ K there is contraction of the first and second coordination spheres. This demonstrates sufficiently high disordering of the oxygen sublattice corresponding to a change of the oxygen migration mechanism. At $T > 3100$ K, the $g_{\text{o–o}}(r)$ behavior reflects the entirely liquid-like state, namely UO_2 melt.

Comparison of the results received in this work with experimental data (Table 2) for the oxygen diffusion coefficients in UO_2 demonstrates that, within the limits of errors, both the diffusion activation energy and the pre-exponential factor of the oxygen diffusion coefficient in the crystalline UO_2 coincide with the experiment.

We consider the mechanism of the transport processes in the model crystals to be the following. The most typical type of disordering in superionic crystals such as UO_2 is the anti-Frenkel disordering, which consists in the formation of interstitial oxygen ions and oxygen vacancies with equal concentrations $C_{\text{Oi}} = C_{\text{Ov}}$. The disordering is characterized by the anti-Frenkel pair formation energy $\Delta E^{\text{O}}_{\text{F}}$ and can be described by the quasi-chemical reaction

$$C_{\text{Oi}} \cdot C_{\text{Ov}} = K^{\text{O}}_{0\text{F}} \exp\{-\Delta E^{\text{O}}_{\text{F}}/kT\}. \tag{6}$$

The effective oxygen diffusion coefficient measured experimentally can be written as

$$D^{\text{O}}_{\text{eff}} = C_{\text{Oi}} \cdot D_0 \exp\{-\Delta E^{\text{D}}_{\text{Oi}}/kT\}. \tag{7}$$

Here, $\Delta E^{\text{D}}_{\text{Oi}}$ is the activation energy of oxygen migration. Consequently, the effective oxygen diffusion activation energy is

$$\Delta E^{\text{O}}_{\text{eff}} = \frac{1}{2}\Delta E^{\text{O}}_{\text{F}} + \Delta E^{\text{D}}_{\text{Oi}}. \tag{8}$$

According to the experimental data, $\Delta E^{\text{D}}_{\text{Oi}} = (0.8–1.0)$ eV, corresponding to the interstitialcy mechanism of migration. Also, $\Delta E^{\text{O}}_{\text{F}} = (3.5 \pm 0.5)$ eV, which within the error limits gives $\Delta E^{\text{O}}_{\text{eff}} = 2.65$ eV coinciding with the experimental value [9,10] and also with the data obtained in this work (No. 1 in Table 2).

Hence, in stoichiometric uranium dioxide the most probable mechanism of oxygen diffusion for the crystalline phase is the interstitialcy migration of interstitial oxygen

Table 2
Parameters of the high-temperature oxygen diffusion in uranium dioxide

No.	Temperature T (K)	$D_{0\text{eff}}$ (cm^2 s^{-1})	$\Delta E^{\text{O}}_{\text{eff}}$, (eV)	Phase state
1	2280–2580	$(0.32^{+0.50}_{-0.11})$	2.76 ± 0.32	Crystal, bulk, present work
2	1800–2600	$(0.8^{+2.9}_{-0.2})$	2.6 ± 0.2	Crystal [2], periodic border conditions
3	1053–1523	0.26	2.6	Crystal, experiment [10], Marin, Contamin
4	1100–1500	1.44	2.74	Crystal, experiment [9], Matzke
5	2300–3007	$(1.8^{+4.8}_{-1.3}) \times 10^{-3}$	2.0 ± 0.3	Crystal, near-surface layer present work
6	2300–3007	$(8.0^{+21.0}_{-5.8}) \times 10^{-3}$	1.63 ± 0.31	Crystal, surface layer present work
7	2624–3000	$(4.4^{+12}_{-3.6}) \times 10^{-2}$	2.34 ± 0.43	Superionic state, bulk present work
8	2600–3100	$(2.6^{+1.9}_{-1.1}) \times 10^{-2}$	1.88 ± 0.13	Superionic state [2], periodic border conditions
9	3120–3680	$(2.0^{+4.3}_{-1.5}) \times 10^{-3}$	1.24 ± 0.32	Melt, present work
10	3100–3600	$(6.6^{+7.6}_{-3.5}) \times 10^{-4}$	0.8 ± 0.2	Melt [2], periodic border conditions

ions formed due to the thermal anti-Frenkel disordering. Reduction of ΔE^{O}_{eff} in the superionic phase (No. 7 in Table 2) can be caused either by decrease of ΔE^{O}_{F} and ΔE^{D}_{Oi} under the same migration mechanism or by the change from the interstitialcy to the vacancy mechanism of migration of oxygen ions.

For the near-surface and surface zones, the activation energies of oxygen diffusion have amounted (2.0 ± 0.3) eV and (1.63 ± 0.31) eV, accordingly. These values are lower than the bulk oxygen diffusion activation energy in the superionic phase, which allows us to assume that, within the whole studied temperature interval, oxygen ions in these two zones remain in the disordered (superionic) state.

At temperatures corresponding to the melt ($T > 3100$ K), the activation energies of oxygen diffusion for all the three crystal zones are equal within the experimental error. The values practically coincide with the activation energy of oxygen diffusion in the nanocrystal surface layer corresponding to the region with $T < T_{melt}$. This confirms disordering of the oxygen sublattice in the surface layer within whole studied temperature interval.

The data on the uranium diffusion coefficients in UO_2 nanocrystals for all the three zones in the temperature range (2624–3950) K are shown in Fig. 6. The dependences of the diffusion coefficients on temperature within the limits

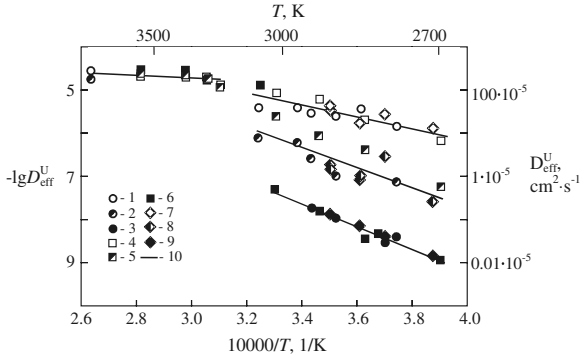

Fig. 6. Dependences of the uranium diffusion coefficients on temperature. 1, 4, 7 – crystal surface zone; 2, 5, 8 – the near-surface zone; 3, 6, 9 – the bulk zone; 1–6 – 6144 ions; 7–9 – 4116 ions; 1–3 – fractional charges, $q_{-} = -1.9085e$; 4–9 – integer charges, $q_{-} = -2e$; and 10 – approximations.

of error can be described by the Arrhenius Eq. (5). The corresponding values of D_{0eff} and ΔE^{U}_{eff} are given in Table 3, along with the results of experiments conducted by other authors. The behavior of the pair radial function for uranium ions indicates the presence of the crystalline phase in the crystal bulk up to the melting temperature $T = 3100$ K. There are characteristic narrow lines of $g_{u-u}(r)$ for the corresponding coordination spheres at $T = 300$ K. Broadening of the peaks at higher temperatures (2500 K and 3000 K) and melting of the UO_2 nanocrystal after 3100 K are also observed. Differences in the character of the $g_{u-u}(r)$ function before and after the superionic transition at $T = 2500$ K and $T = 3000$ K correspondingly, are small, indicating, that in comparison with oxygen the disordering of the uranium sublattice in the bulk zone is low.

The calculated value of the activation energy of the uranium diffusion is (5.0 ± 0.3) eV (No. 1 in Table 3). It is in agreement with experimental value of 5.6 eV (([11]), (No. 3 in Table 3)). Calculated value of the pre-exponential factor is $(3.9^{+9.3}_{-2.8})$ cm^2/s (No. 1 in Table 3), being somewhat higher than the experimental value of 0.65 cm^2/s (([11]), (No. 3 in Table 3)). The divergence can be connected either with errors of the modeling or with the difference of the temperature intervals, where the calculations and the measurements were conducted. In the near-surface and surface zones the calculated activation energies of the uranium diffusion decrease down to (4.4 ± 0.9) eV and (2.8 ± 0.4) eV, accordingly. This indicates essential disordering of these zones. After melting the calculated activation energy of uranium diffusion decreases further, to (0.73 ± 0.36) eV. The values of the activation energies and the pre-exponential factors for the uranium diffusion coefficients acquired in this work within the limits of errors coincide with data received for the crystalline phase and the melt using integer ion charges and periodic border conditions [2] using the experimental dependence of the lattice parameter on temperature (No. 2 in Table 3).

The analysis of the high-temperature uranium diffusion mechanism can be carried out in the same way as for oxygen. The equation for the concentration of the native thermal defects in stoichiometric uranium dioxide must now include in addition to Eq. (6) the concentrations of the interstitial uranium ions C_{Ui} and oxygen and uranium vacancies (C_{Ov}, C_{Uv}). Values of these concentrations are

Table 3
Parameters of the high-temperature uranium diffusion in uranium dioxide

No.	Temperature T (K)	D_{0eff} (cm^2 s^{-1})	ΔE^{U}_{eff}, (eV)	Phase state
1	2624–3000	$3.9^{+9.3}_{-2.8}$	5.0 ± 0.3	Crystal, bulk, present work
2	2600–3100	$(0.25^{+5.04}_{-0.24})$	5.0 ± 0.8	Crystal, periodic border conditions [2]
3	1900–2500	0.65	5.6	Crystal, experiment [9], Matzke
4	2624–3180	$11.7^{+417}_{-11.4}$	4.4 ± 0.9	Crystal, near-surface layer present work
5	2624–3180	$4.4^{+22}_{-3.7}$	2.8 ± 0.4	Crystal, surface layer present work
6	3330–3950	$(4.6^{+1.1}_{-3.2}) \times 10^{-3}$	0.73 ± 0.36	Melt, present work
7	3100–3600	$(5.0^{+10.0}_{-3.0}) \times 10^{-4}$	0.9 ± 0.3	Melt, periodic border conditions [2]

determined by equations of the Frenkel disordering in the uranium sublattice with the formation energy ΔE_F^U and of the Schottky disordering with the energy ΔE_S. The equations can be written as follows:

$$C_{Ui} \cdot C_{Uv} = K_{0F}^U \exp\{-\Delta E_F^U/kT\}, \quad (9)$$

$$C_{Uv} \cdot C_{Ov}^2 = K_{0S}^U \exp\{-\Delta E_S/kT\}. \quad (10)$$

The equation for the coefficients of uranium diffusion via cationic vacancies is

$$D_{eff}^U = C_{Uv} \cdot D_{Uv} = C_{Uv} \cdot D_{Ov} \exp\{-\Delta E_v^D/kT\}, \quad (11)$$

where ΔE_v^D is the vacancy migration energy, D_{0v} is the pre-exponential factor of diffusion coefficient of the vacancies.

From Eqs. (9) and (10) and the equality $C_{Oi} = C_{Ov}$, it follows, that

$$D_{eff}^U = C_{Ov} \cdot D_{Ov} \exp\{-(\Delta E_{eff}^U)/kT\}. \quad (12)$$

Here, ΔE_{eff}^U is the effective activation energy of uranium ion diffusion, given by

$$\Delta E_{eff}^U = \Delta E_S - \Delta E_F^O + \Delta E_v^D. \quad (13)$$

In accordance with the data of experimental and computational work [1,11], values of the activation energies are $\Delta E_S = (6.5 \pm 0.5)$ eV, $\Delta E_F^O = 2.5$ eV,$\Delta E_F^O = (3.5 \pm 0.5)$ eV, giving $\Delta E_{eff}^U = 5.5$ eV. The latter value is in quite good agreement with the result of (5.0 ± 0.3) eV acquired in the present work and with the experimental value of 5.6 eV [11], which indicates diffusion of the uranium cations via the native cationic vacancies.

4. Conclusion

Thus, the comparison with the experimental data indicates the efficiency of the suggested molecular dynamics model in simulations of the transport of uranium and oxygen ions in uranium dioxide nanocrystals and the determination of its characteristics. The temperature dependences obtained for the diffusion coefficients in the bulk and on the surface of the nanocrystals as well as the method of molecular dynamics itself can be used for prediction of the agglomeration and recrystallization processes in uranium dioxide, including processes involving nanocrystals.

References

[1] N.D. Morelon, D. Ghaleb, J.M. Delaye, L. Van Brutzel, Philos. Mag. 83 (2003) 1533.
[2] A.Ya. Kupryazhkin, A.N. Zhiganov, D.V. Risovany, V.D. Risovany, V.N. Golovanov, Tech. Phys. 49 (2004) 254.
[3] K. Kurosaki, K. Yamada, M. Uno, S. Yamanaka, K. Yamamoto, T. Namekawa, J. Nucl. Mater. 294 (2001) 160.
[4] A.V. Fedotov, V.F. Petrunin, V.B. Malygin, V.V. Shilov, Mater. Sci. New Mater. 62 (2) (2006) 207.
[5] J.R. Walker, C.R.A. Catlow, J. Phys. C, Solid State Phys. 14 (1981) L979.
[6] D.M. Skorov, Yu.F. Bychkov, A.I. Dashkovskyi, Reactornoe Materialovedenie, Atomizdat, Moscow, 1979.
[7] J.K. Fink, J. Nucl. Mater. 279 (2000) 1.
[8] V.A. Ryabov, Phys. Rev. E 64 (2001) 64.
[9] Hj. Matzke, in: O.T. Sorensen (Ed.), Diffusion in Nonstoichiometric Oxides, New York, 1981, p. 155.
[10] J.F. Marin, P. Contamin, J. Nucl. Mater. 30 (1969) 16.
[11] Hj. Matzke, J. Chem. Soc., Faraday Trans. II 83 (1987) 1121.